



IJRASET

International Journal For Research in
Applied Science and Engineering Technology



INTERNATIONAL JOURNAL FOR RESEARCH

IN APPLIED SCIENCE & ENGINEERING TECHNOLOGY

Volume: 6

Issue: II

Month of publication: February 2018

DOI:

www.ijraset.com

Call:  08813907089

E-mail ID: ijraset@gmail.com

Heat and Mass Transfer Effects on MHD Boundary Layer Flow of Casson Fluid over an Exponentially Stretching Surface

P. Sreehari Reddy¹, M. Sivaiah²

^{1,2}Department of Mathematics, N.B.K.R. Science and Arts College, SPSR Nellore

Abstract: Heat and mass transfer effects on MHD three dimensional flow of Casson fluid over an exponentially stretching surface with slip conditions is examined. The similarity transformations are used to convert the governing equations into a set of nonlinear ordinary differential equations and are solved numerically using fourth order Runge-Kutta method along with shooting technique. The effects of Casson parameter, Hartmann number, heat source/sink, chemical reaction and slip factors on velocity, temperature and concentration are shown graphically. The skin friction coefficient and the Nusselt number are examined numerically.

Keywords: MHD, Casson parameter, three dimensional flow, slip factors

I. INTRODUCTION

The study of boundary layer flow by stretching surface is related in industrial and engineering applications such as drawing of copper wires, condensation process, die forging and extrusion of polymer in melt spinning, metal extrusion, paper production and fiber production. Prabhakar et al. [1] studied effects of inclined magnetic field and chemical reaction on flow of a Casson Nanofluid with second order velocity slip and thermal slip over an exponentially stretching sheet. Hayat et al. [2] reported on diffusion of chemically reactive species in third grade fluid flow over an exponentially stretching sheet considering magnetic field effects. Giresha et al. [3] investigate MHD three dimensional double diffusive flow of Casson nanofluid with buoyancy forces and nonlinear thermal radiation over a stretching surface. Sharma et al. [4] presented on MHD slip flow and heat transfer over an exponentially stretching permeable sheet embedded in a porous medium with heat source. Nadeem et al. [5] discussed non aligned stagnation point flow of radiating Casson fluid over a stretching surface. Tasawar Hayat et al. [6-8] developed radiative three dimensional flow with sores and dufour effects. MHD stagnation point flow accounting variable thickness and slip conditions and three dimensional flow of CNTs nanofluids with heat generation/absorption effect: A numerical study.

Krishna Murthy [9] studied MHD three dimensional flow of Jeffrey fluid over an exponentially stretching sheet. MHD three dimensional flow by an exponentially stretching surface with convective boundary condition was analyzed by Hayat et al. [10]. Nayak et al. [11] established three dimensional MHD flow of nanofluid over an exponential porous stretching sheet with convective boundary conditions. Tasawar Hayat et al. [12-15] addressed sores and dufour effects in three dimensional flow over an exponentially stretching surface with porous medium, chemical reaction and heat source/sink. Three dimensional mixed convection flow of viscoelastic nanofluid over an exponentially stretching surface. Thermally stratified stagnation point flow of Casson fluid with slip conditions and three dimensional flow of Eyring Powel nanofluid over an exponentially stretching sheet. Chung Liu et al. [16] developed flow and heat transfer for three dimensional flow over an exponentially stretching surface. Magyari et al. [17] examined Heat and mass transfer in the boundary layer on an exponentially stretching continuous surface. Butt et al. [18] obtained three dimensional flow of a magneto hydrodynamic Casson fluid over an unsteady stretching sheet embedded into a porous medium. Hayat et al. [19-20] discussed Unsteady MHD flow over exponentially stretching sheet with slip conditions and MHD flow of Casson fluid over a stretching cylinder. The present study slip effects on MHD three dimensional flow of Casson fluid over an exponentially stretching surface. The governing equations are solved numerically using fourth order Runge- Kutta method along with shooting technique. The effects of governing parameters on velocity, temperature, concentration obtained graphically. The skin friction coefficient and nusselt number are examined numerically.

II. MATHEMATICAL FORMULATION OF THE PROBLEM

Consider the steady three dimensional flow of Casson fluid over an exponentially stretching surface. The sheet is stretched along the xy -plane while fluid is placed along the z -axis. Moreover the constant magnetic field is applying normal to the fluid flow and the

induced magnetic field assumed to be negligible. The sheet at $z = 0$ is stretched in the x - and y -directions with velocities U_w and V_w respectively. The rheological equation of state for an isotropic flow of a Casson fluid can be expressed as follows

$$\tau_{ij} = \begin{cases} 2\left(\mu_B + \frac{p_z}{\sqrt{2\pi}}\right) e_{ij}, & \pi > \pi_c \\ 2\left(\mu_B + \frac{p_z}{\sqrt{2\pi}}\right) e_{ij}, & \pi < \pi_c \end{cases} \quad (1)$$

in the above equation $\pi = e_{ij}$ and e_{ij} denotes the $(i, j)^{th}$ component of the deformation rate, π be the product of the component of deformation rate itself, π_c be a critical value of this product based on the non-Newtonian model, μ_B be the plastic dynamic viscosity of the Casson fluid and p_z be the yield stress of the fluid. The governing boundary layer equations are as follows

$$\frac{\partial u}{\partial x} + \frac{\partial v}{\partial y} + \frac{\partial w}{\partial z} = 0 \quad (2)$$

$$u \frac{\partial u}{\partial x} + v \frac{\partial u}{\partial y} + w \frac{\partial u}{\partial z} = \nu \left(1 + \frac{1}{\beta}\right) \frac{\partial^2 u}{\partial z^2} - \frac{\sigma B_0^2}{\rho} u \quad (3)$$

$$u \frac{\partial v}{\partial x} + v \frac{\partial v}{\partial y} + w \frac{\partial v}{\partial z} = \nu \left(1 + \frac{1}{\beta}\right) \frac{\partial^2 v}{\partial z^2} - \frac{\sigma B_0^2}{\rho} v \quad (4)$$

$$u \frac{\partial T}{\partial x} + v \frac{\partial T}{\partial y} + w \frac{\partial T}{\partial z} = \alpha_m \frac{\partial^2 T}{\partial z^2} + \frac{Q}{\rho c_p} (T - T_\infty) \quad (5)$$

$$u \frac{\partial C}{\partial x} + v \frac{\partial C}{\partial y} + w \frac{\partial C}{\partial z} = D \frac{\partial^2 C}{\partial z^2} - K_1 (C - C_\infty) \quad (6)$$

where u, v and w are the velocity components corresponding to x -, y - and z - directions respectively. ρ is the fluid density, B_0 is the magnetic field of strength, ν is the kinematic viscosity, β is the Casson parameter, σ is the electrical conductivity of fluid, α_m is the thermal diffusivity, Q is the heat generation/absorption parameter, c_p is the specific heat, T is represents the temperature of fluid, D is the diffusion coefficient, C is the concentration, K_1 is the reaction rate, C_∞ is the concentration far away from the surface and T_∞ is the temperature far away from the surface.

The associated with boundary conditions of equations (2)-(6) at the wall can be expressed as

$$\left. \begin{aligned} u = U_w = U_0 e^{\frac{x+y}{L}}, v = V_w = V_0 e^{\frac{x+y}{L}} \\ w = 0, T = T_w = T_\infty + T_0 e^{A\left(\frac{x+y}{2L}\right)} + L_1 \frac{\partial T}{\partial z}, C = C_w = C_\infty + C_0 e^{B\left(\frac{x+y}{2L}\right)} + L_2 \frac{\partial T}{\partial z} \end{aligned} \right\} \text{at } z = 0 \quad (7a)$$

$$u = 0, v = 0, T \rightarrow T_\infty, C \rightarrow C_\infty \text{ as } z \rightarrow \infty \text{ (7b)}$$

where U_w and V_w are the stretching velocities, U_0, T_0, C_0 and V_0 are constants, A and B are the temperature and concentration exponents, T_w is the surface temperature, T_0 is the reference temperature, T_∞ is the ambient temperature, L_1 and L_2 are temperature and concentration slip factors and L is the reference length.

In order to transform equations (2)-(7) to the dimensionless form, the following transforms are applied

$$\left. \begin{aligned} u = U_0 e^{\frac{x+y}{L}} f'(\eta), v = V_0 e^{\frac{x+y}{L}} g'(\eta), w = -\left(\frac{\nu U_0}{2L}\right)^{\frac{1}{2}} e^{\frac{x+y}{L}} (f + \eta f' + g + \eta g') \\ \theta(\eta) = \frac{T - T_\infty}{T_0 e^{\frac{A(x+y)}{2L}}}, \phi(\eta) = \frac{C - C_\infty}{C_0 e^{\frac{B(x+y)}{2L}}}, \eta = \left(\frac{U_0}{2\nu L}\right)^{\frac{1}{2}} e^{\frac{x+y}{2L}} z \end{aligned} \right\} \text{ (8)}$$

where η is the similarity variable. Substituting equation (8) in (3)-(7) equation (2) is satisfied automatically and equations (3)-(7) are reduced to the following nonlinear ordinary differential equations

$$\left(1 + \frac{1}{\beta}\right) f''' - 2(f' + g')f' + (f + g)f'' - M^2 f' = 0 \text{ (9)}$$

$$\left(1 + \frac{1}{\beta}\right) g''' - 2(f' + g')g' + (f + g)g'' - M^2 g' = 0 \text{ (10)}$$

$$\theta'' + \text{Pr}[(f + g)\theta' - A(f' + g')\theta + S\theta] = 0 \text{ (11)}$$

$$\phi'' + \text{Sc}[(f + g)\phi' - B(f' + g')\phi - \gamma\phi] = 0 \text{ (12)}$$

the transformed boundary conditions can be written as

$$\left. \begin{aligned} f(0) = 0, f'(0) = 1, g(0) = 0, g'(0) = \alpha, \theta(0) = 1 + \gamma_1 \theta'(0), \phi(0) = 1 + \gamma_2 \phi'(0) \\ f'(\infty) \rightarrow 0, g'(\infty) \rightarrow 0, \theta(\infty) \rightarrow 0, \phi(\infty) \rightarrow 0 \end{aligned} \right\} \text{ (13)}$$

where prime denotes the differentiation with respect to the similarity variable η , $M = \frac{\sigma B_0^2 L}{\rho U_w}$ is the Hartmann number, $\text{Sc} = \frac{\nu}{D}$ is

the Schmidt number, $\gamma = \frac{2K_1 L}{U_w}$ is the chemical reaction parameter, $S = \frac{2QL}{U_w \rho c_p}$ is the heat source/sink parameter, A and B are

the temperature and concentration exponent $\text{Pr} = \frac{\nu}{\alpha_m}$ is the Prandtl number, $\alpha = \frac{V_0}{U_0}$ is the ratio parameter, $\gamma_1 = L_1 \left(\frac{U_0 e^x}{\nu L}\right)^{1/2}$

and $\gamma_2 = L_2 \left(\frac{U_0 e^x}{\nu L}\right)^{1/2}$ are the temperature slip parameter and the concentration slip parameter and β is the Casson parameter.

The physical quantities of interest are the skin friction coefficients along the

x - and y -directions are given by

$$C_{fx} = \frac{\mu \left(1 + \frac{1}{\beta}\right) \left(\frac{\partial u}{\partial z}\right)_{z=0}}{\frac{1}{2} \rho U_w^2} \quad \text{and} \quad C_{fy} = \frac{\mu \left(1 + \frac{1}{\beta}\right) \left(\frac{\partial v}{\partial z}\right)_{z=0}}{\frac{1}{2} \rho U_w^2} \quad (14)$$

the skin friction coefficients in dimensionless form are

$$C_{fx} = \left(\frac{\text{Re}_{xy}}{2}\right)^{-1/2} e^{\frac{3(x+y)}{2L}} \left(1 + \frac{1}{\beta}\right) f''(0) \quad \text{and} \quad C_{fy} = \left(\frac{\text{Re}_{xy}}{2}\right)^{-1/2} e^{\frac{3(x+y)}{2L}} \left(1 + \frac{1}{\beta}\right) g''(0) \quad (15)$$

The local Nusselt number Nu_x and local Sherwood number Sh_x are defined as

$$Nu_x = -\frac{x}{T_w - T_\infty} \frac{\partial T}{\partial z} \Big|_{z=0} = -\frac{x}{L} \left(\frac{\text{Re}_{xy}}{2}\right)^{1/2} e^{\frac{(x+y)}{2L}} \theta'(0) \quad (16)$$

$$Sh_x = -\frac{x}{C_w - C_\infty} \frac{\partial C}{\partial z} \Big|_{z=0} = -\frac{x}{L} \left(\frac{\text{Re}_{xy}}{2}\right)^{1/2} e^{\frac{(x+y)}{2L}} \phi'(0) \quad (17)$$

where Re_{xy} is the Reynolds number defined by $\text{Re}_{xy} = \frac{U_w L}{\nu}$.

III. RESULTS AND DISCUSSIONS

The present chapter heat and mass transfer effects on MHD 3dimensional flow of Casson fluid over an exponentially stretching surface with slip conditions is examined. The transformed governing equations are solved numerically using shooting technique. The numerical computations are performed for several values of dimensionless parameters involved in the equations, viz. M is the magnetic parameter, β is the Casson parameter, α is the stretching ratio parameter, Pr is the Prandtl number and A and B are the temperature and concentration exponent. Sc is the Schmidt number, γ is the chemical reaction parameter, S is the heat source/sink parameter, γ_1 and γ_2 are the temperature slip parameter and the concentration slip parameter. The numerical computations have been carried out for various values of the parameters on velocity, temperature and concentration are depicted in figures 1- 10. Variation of Casson parameter β on velocities $f'(\eta)$ and $g'(\eta)$ are shown in figure 1. It is analyzed that the velocity and momentum boundary layer thickness reduces for higher values of Casson parameter. In fact that the large values of Casson parameter then the yield stress decreases which offers less resistance to the fluid motion. Figure 2 depict the impact of magnetic parameter M on velocities $f'(\eta)$ and $g'(\eta)$. It is noticed that an increase in magnetic parameter reduces the fluid velocity and momentum boundary layer thickness. In fact that the magnetic parameter corresponds to an increase in Lorentz force creates a resistance in fluid flow by which the velocity and momentum boundary layer thickness reduces. The influence of ration parameter α on velocity $g'(\eta)$ is shown in figure 3. It can be seen that the velocity and momentum boundary layer thickness increased when ration parameter increases. The lateral surface starts to move in the y -direction when ration parameter increases from zero. This fact the velocity is enhanced. The impact of Prandtl number Pr , temperature exponent A and temperature slip parameter γ_1 on temperature $\theta(\eta)$ are demonstrated in figures 4-6. We observed that the temperature and thermal boundary layer thickness reduces with large

values of Prandtl number, temperature exponent and temperature slip parameter. From figure 4 we note that physically increasing in Prandtl number fluids have weaker thermal diffusivity due to this fact the temperature reduces. The temperature $\theta(\eta)$ reduces with higher values of β is shown in figure 5. An increase in thermal slip parameter the heat transfer from the surface to the adjacent fluid decreases. Therefore temperature of the fluid decrease is displayed in figure 6. The variation of Schmidt number Sc , concentration exponent B , chemical reaction parameter γ and concentration slip parameter γ_2 on concentration $\phi(\eta)$ are shown in figures 7-10. It is obvious that the concentration and concentration boundary layer thickness are decreasing with increasing Schmidt number, concentration exponent, chemical reaction parameter and concentration slip parameter. From figure 7 it is noted that Schmidt number is inversely proportional to the diffusion coefficient. This small diffusion coefficient creates a reduction in concentration when we increase the values of Schmidt number. Concentration increases with increasing in chemical reaction is displayed in figure 8. The smaller values of concentration exponent tends to stronger concentration field is indicates in figure 9. Concentration of the fluid is higher for a small value of concentration slip parameter is shown in figure 10.

The numerical values of the skin friction coefficients $-\left(1 + \frac{1}{\beta}\right)f''(0)$ and $-\left(1 + \frac{1}{\beta}\right)g''(0)$ are displayed in table 1. We have seen that the skin friction coefficients are increasing for higher values of velocity ration parameter α . The rate of heat transfer $\theta'(0)$ is shown in table 2. It is decays via increasing in Prandtl number Pr . Table 1 and Table 2 are displaying the comparing the present results with existing available results in a limiting cases. This tables represent have been good agreement with the previous available results.

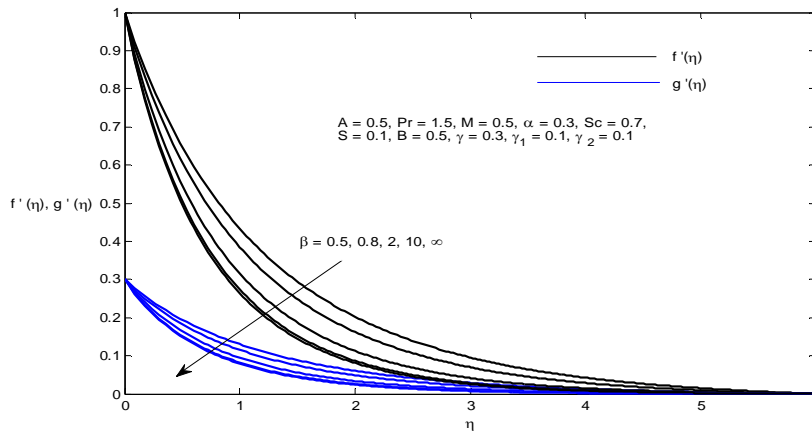


Figure 1. Velocity profiles $f'(\eta), g'(\eta)$ for different values of β

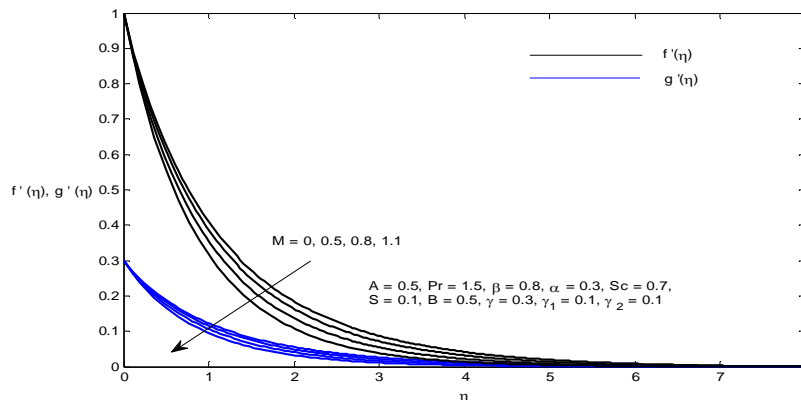


Figure 2. Velocity profiles $f'(\eta), g'(\eta)$ for different values of M

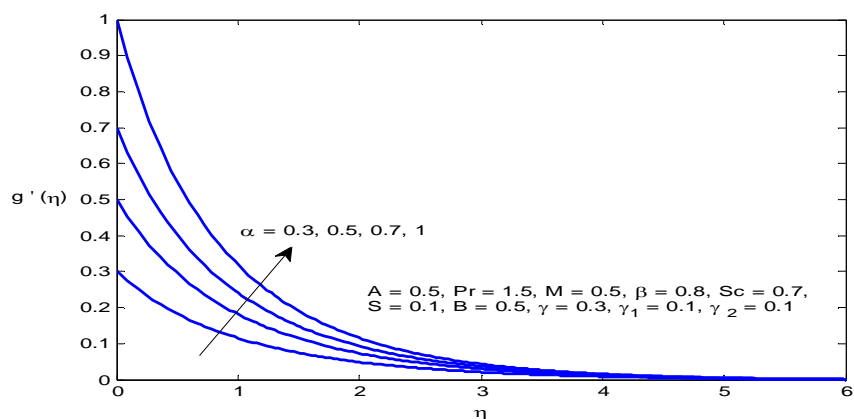


Figure 3. Velocity profiles $g'(\eta)$ for different values of α

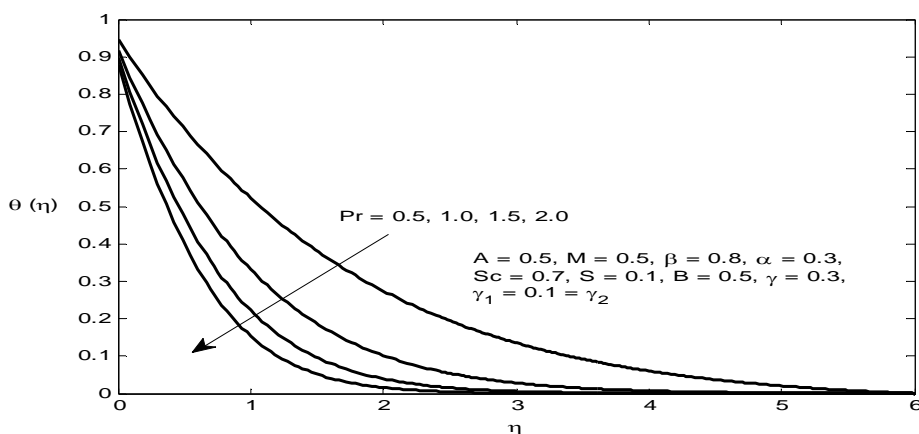


Figure 4. Temperature $\theta(\eta)$ profiles for different values of Pr

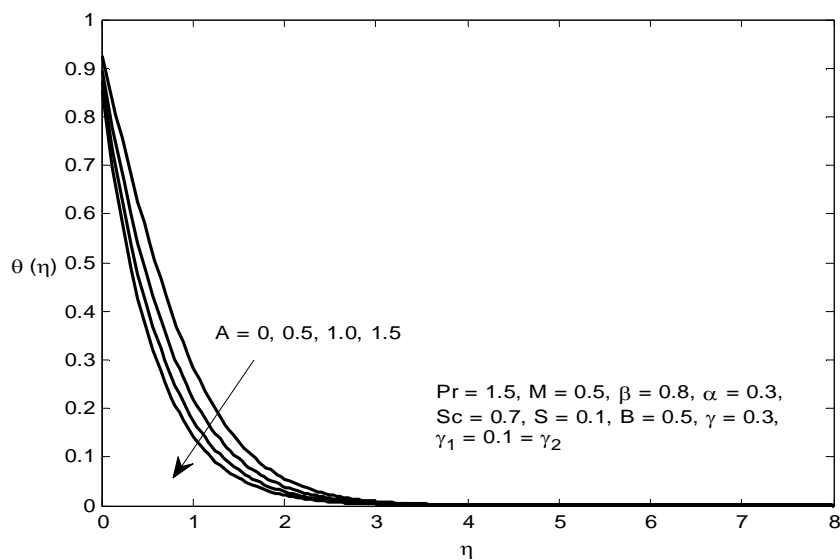


Figure 5. Temperature $\theta(\eta)$ profiles for different values of A

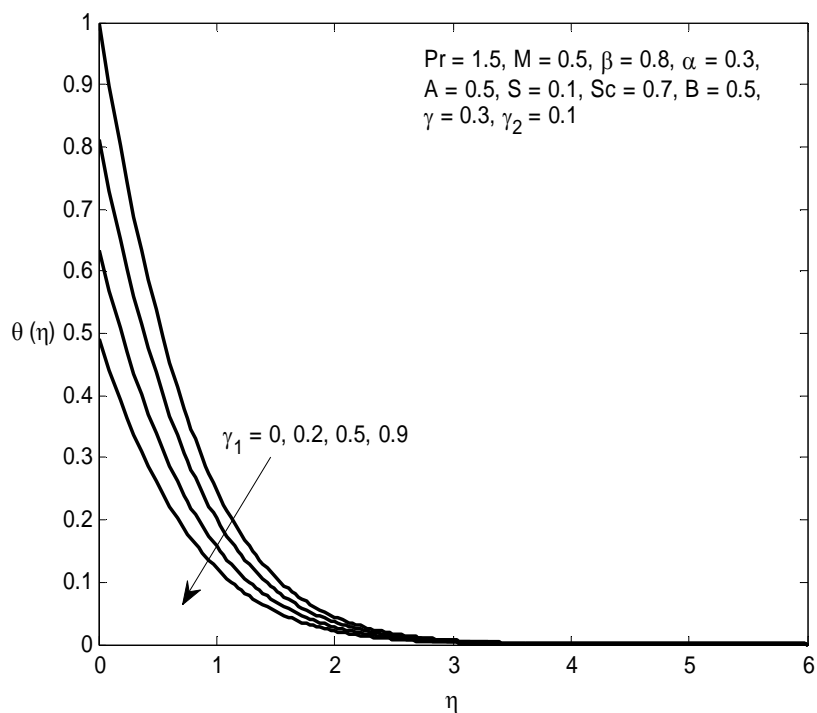


Figure 6. Temperature $\theta(\eta)$ profiles for different values of γ_1

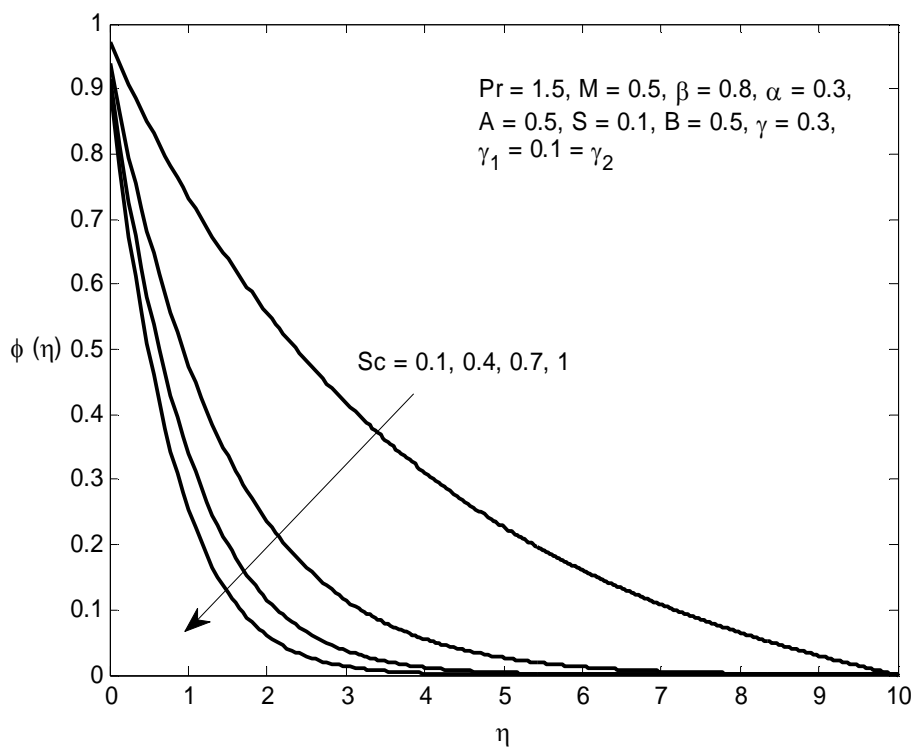


Figure 7. Concentration $\phi(\eta)$ profiles for different values of Sc

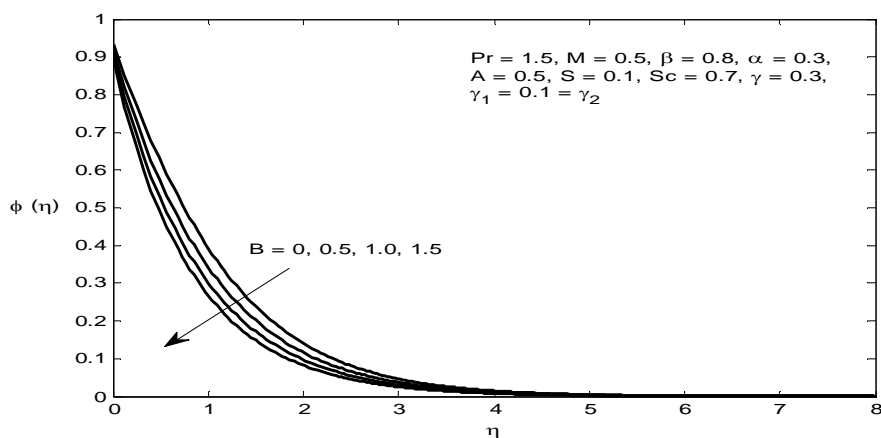


Figure 8. Concentration $\phi(\eta)$ profiles for different values of B

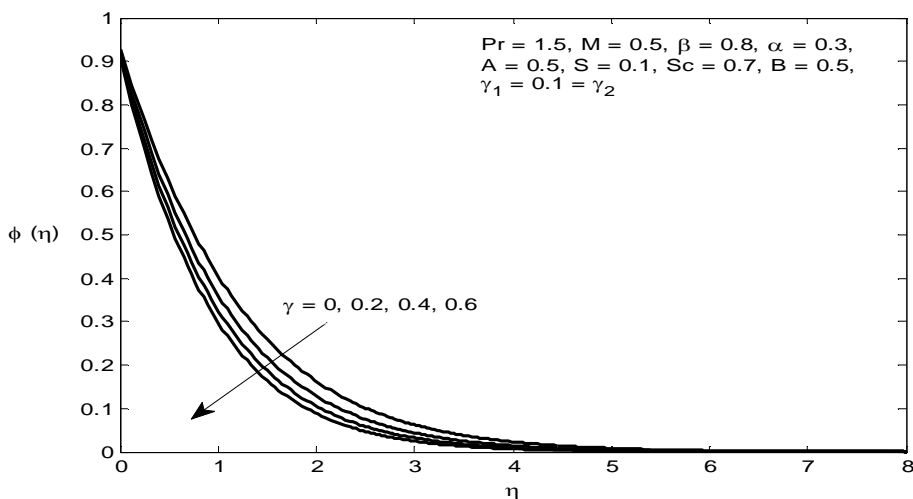


Figure 9. Concentration $\phi(\eta)$ profiles for different values of γ

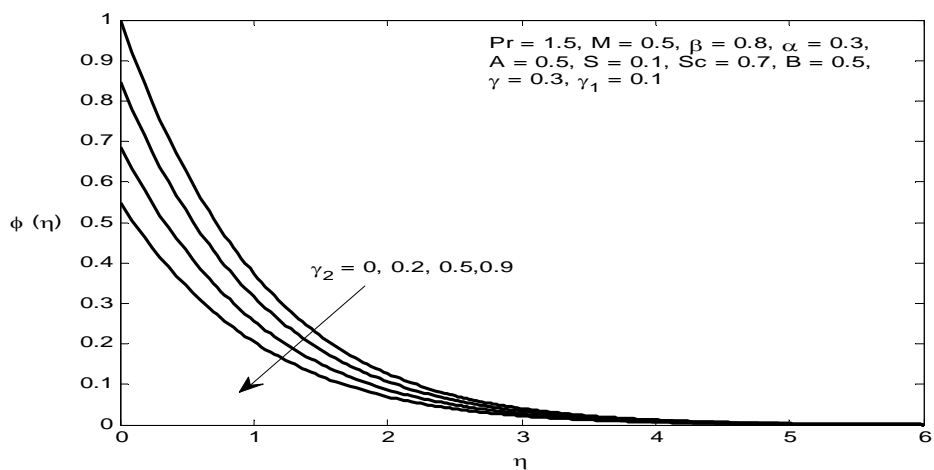


Figure 10. Concentration $\phi(\eta)$ profiles for different values of γ_2

Table 1: comparative table values of $-\left(1+\frac{1}{\beta}\right)f''(0)$ and $-\left(1+\frac{1}{\beta}\right)g''(0)$ for various values of α with $Pr = 0.7, \beta = -2$

when $\beta \rightarrow \infty, \gamma_1 = \gamma_2 = M = S = A = 0$

| α | Liu <i>et al</i> [16], Hayat <i>et al.</i> [12] | | Present results ($\beta \rightarrow \infty, \gamma_1 = \gamma_2 = M = S = A = 0$) | |
|----------|---|------------|--|-----------|
| | $-f''(0)$ | $-g''(0)$ | $-f''(0)$ | $-g''(0)$ |
| 0 | 1.28180856 | 0 | 1.2818114 | 0 |
| 0.5 | 1.56988846 | 0.78494423 | 1.5699104 | 0.7849552 |
| 1.0 | 1.81275105 | 1.81275105 | 1.8127654 | 1.8127654 |

Table 2: comparison of $\theta'(0)$ of Magyari and Keller [17] and Liu *et al.* [16] with the present

study for $\beta \rightarrow \infty, \gamma_1 = \gamma_2 = M = S = \alpha = A = 0$

| Pr | A | $\theta'(0)$ | | |
|----|------|---|---|---|
| | | Magyari & Keller [17] Hayat <i>et al.</i> [12] | Liu <i>et al.</i> [16], Hayat <i>et al.</i> [12] | Present study $\beta \rightarrow \infty, \gamma_1 = \gamma_2 = M = S = \alpha = A = 0$ |
| 1 | -1.5 | 0.377413 | 0.37741256 | 0.3774106 |
| | 0 | -0.549643 | -0.54964375 | -0.5496460 |
| | 1 | -0.954782 | -0.95478270 | -0.9547852 |
| 5 | 3 | -1.560294 | -1.56029540 | -1.5603044 |
| | -1.5 | 1.353240 | 1.35324050 | 1.3532396 |
| | 0 | -1.521243 | -1.52123900 | -1.5212381 |
| 10 | 1 | -2.500135 | -2.50013157 | -2.500704 |
| | 3 | -3.886555 | -3.88655510 | -3.8865583 |
| | -1.5 | 2.200000 | 2.20002816 | 2.2000298 |
| | 0 | -2.257429 | -2.25742372 | -2.2574288 |
| | 1 | -3.660379 | -3.66037218 | -3.6603259 |
| | 3 | -5.635369 | -5.62819631 | -5.6281349 |

REFERENCES

- [1] Beshapu Prabhakar, Shanker Bandari and Kishore kumar Ch, effects of inclined magnetic field and chemical reaction on flow of a Casson Nanofluid with second order velocity slip and thermal slip over an exponentially stretching sheet, International Journal of Applied and Computational Mathematics, Vol. 3, 4, pp. 2967-2985, 2017.
- [2] Hayat T, Ijaz Khan M, Waqas M, Alsaedi A and Yasmeen T, diffusion of chemically reactive species in third grade fluid flow over an exponentially stretching sheet considering magnetic field effects, Chinese Journal of Chemical Engineering, Vol. 25, 3, pp. 257-263, 2017.
- [3] Giresha B J, Archana M, Prasannakumara B C, Reddy Gorla R S, Oluwole Daniel Makinde, MHD three dimensional double diffusive flow of Casson nanofluid with buoyancy forces and nonlinear thermal radiation over a stretching surface, International Journal of Numerical Methods for Heat and Fluid Flow, Vol. 27, 12, pp. 2858-2878, 2017.
- [4] Sharma P R, Sushila Choudary and Makinde O D, MHD slip flow and heat transfer over an exponentially stretching permeable sheet embedded in a porous medium with heat source, Frontiers in Heat and Mass Transfer, Vol. 9, 18, pp.1-7, 2017.
- [5] Rashid Mehmood, Rana S, Akbar N S and Nadeem S, non aligned stagnation point flow of radiating Casson fluid over a stretching surface, Alexandria Engineering Journal, Article in press, 2017.
- [6] Tasawar Hayat, Ikram Ullah, Taseer Muhammad, Ahmed Alsaedi, radiative three dimensional flow with sores and dufour effects, International Journal of Mechanical Sciences, Vol. 133, pp.829-837, 2017.
- [7] Waleed Ahmed Khan, Waqas M, Ijaz Khan, Alsaedi A and Hayat T, MHD stagnation point flow accounting variable thickness and slip conditions, Colloid and Polymer Science, Vol. 295, 7, pp. 1201-1209, 2017.
- [8] Zakir Hussain, Hayat T, Alsaedi A and Ahmad B, three dimensional flow of CNTs nanofluids with heat generation/absorption effect: A numerical study, Computer Methods in Applied Mechanics and Engineering, Vol.329, pp. 40-54, 2017.



- [9] Krishna Murthy M, MHD three dimensional flow of Jeffrey fluid over an exponentially stretching sheet, International Journal for Research in Applied Science and Engineering Technology, Vol. 5, 12, pp. 893-901, 2017.
- [10] Hayat T, Shehzad S A and Alsaedi A, MHD three dimensional flow by an exponentially stretching surface with convective boundary condition, Journal of Aerospace Engineering, pp. 1-8, 2014.
- [11] Nayak M K, Akbar N S, Tripathi D and Pandey V S, three dimensional MHD flow of nanofluid over an exponential porous stretching sheet with convective boundary conditions, Thermal Science and Engineering Progress, Vol.3, pp. 133-140, 2017.
- [12] Tasawar Hayat, Taser Muhammad, Sabir Ali Shehzad and Alsaedi A, sores and dufour effects in three dimensional flow over an exponentially stretching surface with porous medium, chemical reaction and heat source/sink, International Journal of Numerical Methods for Heat and Fluid Flow, Vol. 25, 4, pp. 762-781, 2015.
- [13] Tasawar Hayat, Bilal Ashraf, Sabir Ali Shehzad, Alsaedi A and Bayomi N, Three dimensional mixed convection flow of viscoelastic nanofluid over an exponentially stretching surface, International Journal of Numerical Methods for Heat and Fluid Flow Vol. 25, 2, pp. 333-357, 2015.
- [14] Tasawar Hayat, Muhammad Farooq, Alsaedi A, Thermally stratified stagnation point flow of Casson fluid with slip conditions, International Journal of Numerical Methods for Heat and Fluid Flow, Vol. 25, 4, pp. 724-748, 2015.
- [15] Tasawar Hayat, Bilal Ashraf, Sabir Ali Shehzad and Elbaz Abouelmagd, Three dimensional flow of Eyring Powel nanofluid over an exponentially stretching sheet, International Journal of Numerical Methods for Heat and Fluid Flow, Vol. 25, 3, pp. 593-616, 2015.
- [16] Chung Liu I, Hung Hsun Wang and Yih Ferng Peng, flow and heat transfer for three dimensional flow over an exponentially stretching surface, Chemical Engineering Communications, Vol. 200, 2, pp.253-268, 2013.
- [17] Magyari E and Keller B, Heat and mass transfer in the boundary layer on an exponentially stretching continuous surface, J. Phys. D: Appl. Phys, Vol. 32, pp. 577-585, 1999.
- [18] Butt A S, Tufail M N and Asif Ali, three dimensional flow of a magnetohydrodynamic Casson fluid over an unsteady stretching sheet embedded into a porous medium, Journal of Applied Mechanics and Technical Physics, Vol. 57, 2, pp. 283-292, 2016.
- [19] Hayat T, Shafiq A, Alsaedi A and Shahzad S A, Unsteady MHD flow over exponentially stretching sheet with slip conditions, Applied Mathematics and Mechanics, Vol. 37, 2, pp.193-208, 2016.
- [20] Tamoor M, Waqas M, Ijaz Khan M, Ahmed Alsaedi, Hayat T, MHD flow of Casson fluid over a stretching cylinder, Results in Physics, Vol. 7, pp. 498-502, 2017.



10.22214/IJRASET



45.98



IMPACT FACTOR:
7.129



IMPACT FACTOR:
7.429



INTERNATIONAL JOURNAL FOR RESEARCH

IN APPLIED SCIENCE & ENGINEERING TECHNOLOGY

Call : 08813907089  (24*7 Support on Whatsapp)